Letter

When Flexoelectricity Drives Triboelectricity

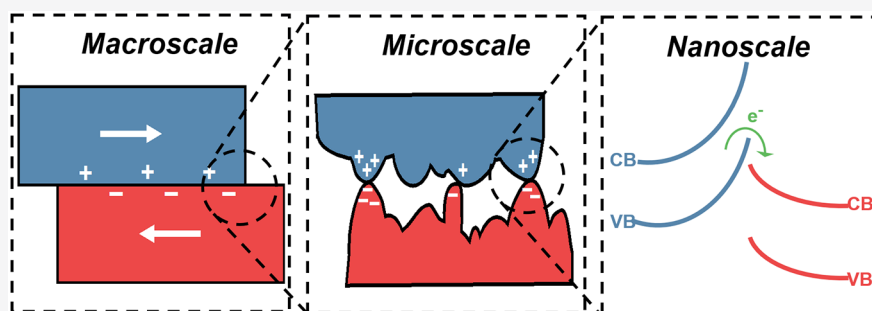Christopher A. Mizzi and Laurence D. Marks*

ACCESS | Metrics & More | Article Recommendations | Supporting Information

ABSTRACT: Triboelectricity has been known since antiquity, but the fundamental science underlying this phenomenon lacks consensus. We present a flexoelectric model for triboelectricity where contact deformation induced band bending at the nanoscale is the driving force for charge transfer. This framework is combined with first-principles and finite element calculations to explore charge transfer implications for different contact geometry and materials combinations. We demonstrate that our *ab initio* based formulation is compatible with existing empirical models and experimental observations including charge transfer between similar materials and size/pressure dependencies associated with triboelectricity.

KEYWORDS: Flexoelectricity, Triboelectricity, Tribology, Band Bending, Contact Mechanics

Triboelectricity, the charge transfer associated with contacting and rubbing two materials, has been known for at least 25 centuries.[1,2] It can be a boon or a bane in industries[3] ranging from xerography[4] to pharmaceuticals[5] and is thought to play a critical role in many processes such as dust storms[6] and planetary formation.[7] To date, a consensus on the fundamental science of triboelectricity including the driving force and transferred charged species has proven elusive. For metal-on-metal contact, charging is generally accepted to be in part associated with electron transfer driven by contact potential differences.[8] The literature is less clear for metal-on-insulator and insulator-on-insulator contacts, with experiments suggesting a variety of charged species[1-3,9] and models invoking several mechanisms such as temperature differences[10] and trapped charges.[11,12]

As demonstrated first by Bowden and Tabor,[13] friction and wear at the nanoscale are due to adhesion between as well as elastic deformation of nanoscale asperities. The macroscopic friction one observes is due to the variations in the statistical number of nanoscale contacts with load, not a fundamental materials property. Asperities have been considered in triboelectricity; for instance, Volta and Helmholtz[14-16] hypothesized that the role of rubbing in tribocharging was to increase the number of contact points between two materials, while Harper in 1967 in his classic monograph[17] stressed the importance of considering asperity contact, arguing that somehow they played a major role. Similar to friction,

macroscopic charging will be a statistical average over local charge mosaics.[18] It has also been shown that *macroscopic* deformations play an important role in triboelectricity (first in 1910 when bending was found to dictate the direction of charge transfer[19] with further work over the next century[20-23]). Until recently there has been no model to explain the link between such deformations and triboelectricity based upon *ab initio* quantum mechanics.

We recently analyzed these deformations using flexoelectricity,[24] the electromechanical coupling between polarization and strain gradient present in all insulators.[25] In that work we demonstrated that elastic strain fields at contacting asperities generate potential differences via the flexoelectric effect that are large enough to drive charge transfer for typical rubbing or contact conditions. Our model was found to be consistent with many experimental observations including charge mosaics,[18] bipolar charging during stick–slip,[26] and curvature dependences,[27] with no adjustable parameters beyond material properties, and an independent expansion of this model to
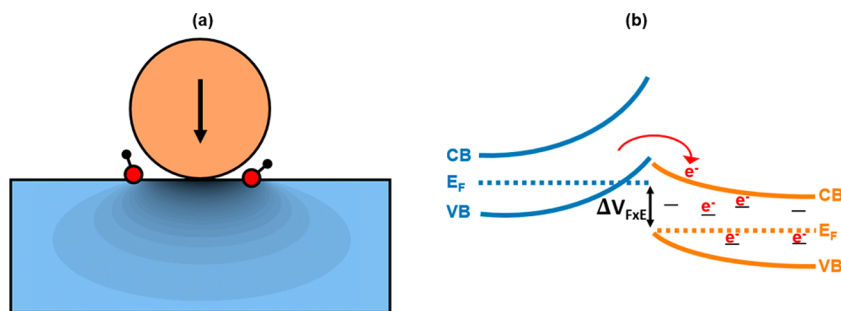
Figure 1. (a) Schematic of sphere-on-flat contact depicting elastic deformation fields emanating from the contact point and adsorbed species on the surface. (b) Elastic deformations induce an additional contact potential term through flexoelectric couplings. Depending on the materials, geometry, and extent of deformation, contact-induced band bending can drive the occupation of trap states, bulk charge transfer, or the adsorption of charged species.

randomly rough surfaces has also shown good agreement with experiment.[28]

While the simplifying assumptions made in ref 22 were sufficient to address the basic physics of triboelectricity and make qualitative comparisons with experiments, they are inadequate for quantitative analysis and do not explain several known phenomena. First, only the effects of the electric field component normal to the contact interface were considered, which must be revised to calculate quantitative band bending profiles. Second, Hertz theory was assumed which would lead to no tribocharging between chemically identical materials, in conflict with experimental results. Third, the work in ref 22 was not rooted in band structure theory, so it could not rigorously explain the work function dependency of tribocharging in insulators[29,30] or the role of trap states.[11,12] Additionally, it could not explain the change in the sign and magnitude of charge transfer with pressure[16,31] as well as some other experimental results.

In this letter, we extend and generalize the flexoelectric model for triboelectric charging by including the specifics of band bending. We show that flexoelectricity-driven band bending during nanoscale contact between different/like materials is a mechanical analogue of traditional band bending in hetero/homojunctions in semiconductor devices; transfer of charge during contact can be thought of as a contact-driven diode. Our findings are consistent with existing empirical models involving trap states, contact potentials, and ion transfer, but now these dependencies arise naturally from an *ab initio* based formulation of the problem. Of particular importance, the results indicate charge transfer between two materials in contact can act as either a conventional or a Zener/breakdown diode depending upon both the material and the magnitude of the contact force. This explains variations in both the sign and the magnitude of charge transfer with force, a key experimental observation which to our knowledge has been unexplained.

As illustrated in Figure 1, elastic deformations induce band bending around a contact point. A description of such electronic structure changes (within the Schottky−Mott limit of no charge transfer[32,33]) corresponds to determining the spatial variation of the conduction band (CB) and valence band (VB) edges in each contacting body with deformation. In a centrosymmetric insulator subjected to an inhomogeneous strain, the change in the energy of a band feature E_i referenced to vacuum E_{vac} is

$$\Delta(E_i(\mathbf{r}) - E_{vac}(\mathbf{r})) = \Delta\overline{V}_{FxE}(\mathbf{r}) + (\varphi + D_i)\epsilon(\mathbf{r}) \qquad (1)$$

The first term $\Delta\overline{V}_{FxE}(\mathbf{r})$ corresponds to the change in the average Coulomb potential arising from strain gradients via the bulk flexoelectric effect. Other electromechanical couplings are not considered because piezoelectricity is a bulk property only in a subset of materials[34] and known to be insufficient to explain triboelectricity,[1] whereas flexoelectricity is important at the nanometer length scales relevant to asperity contact due to the intrinsic size-dependence of strain gradients.[25] $\Delta\overline{V}_{FxE}(\mathbf{r})$ in eq 1 is given by

$$\Delta\overline{V}_{FxE}(\mathbf{r}) = \overline{V}(\mathbf{r}) - \overline{V}_0$$
$$= \frac{1}{4\pi\epsilon_0(1 + \chi)} \int_\Omega \frac{\mathbf{P}_{FxE}(\mathbf{r}')\cdot(\mathbf{r} - \mathbf{r}')}{|\mathbf{r} - \mathbf{r}'|^3}\, d\Omega' \qquad (2)$$

where $\overline{V}(\mathbf{r})$ is the average Coulomb potential at point $\mathbf{r}$ in the deformed body referenced to $\overline{V}_0$, the average Coulomb potential sufficiently far from the contact point, ϵ_0 is the permittivity of free space, χ is the dielectric susceptibility, and $\mathbf{P}_{FxE}(\mathbf{r}')$ is the flexoelectric polarization at point $\mathbf{r}'$. The second term φ gives the shift in the average Coulomb potential with respect to vacuum (also known as the mean-inner potential) induced by strain ϵ.

$$\varphi = \frac{d(\overline{V} - E_{vac})}{d\epsilon} \qquad (3)$$

This term enables a direct comparison between different materials by introducing an absolute energy reference and implicitly includes "surface" flexoelectric effects;[35,36] see ref 36 for a more comprehensive analysis of this including the effects of different surface structures. The third term $D_i(\mathbf{r})$ describes the relative deformation potential, i.e., the local change in energy of a band feature relative to the average Coulomb potential from strain.[37,38]

$$D_i = \frac{d(E_i - \overline{V})}{d\epsilon} \qquad (4)$$

The relative offset between two materials, A and B, in contact can be found by combining eq 1 for each material with their work function difference $(\Delta\phi)$ according to

$$\Delta(E_{VBM}^A(\mathbf{r}) - E_{vac}^A(\mathbf{r})) = \Delta(E_{VBM}^B(\mathbf{r}) - E_{vac}^B(\mathbf{r})) + \Delta\phi \qquad (5)$$

Here, the valence band maximum is the relevant band feature owing to the definition of the work function.

To explore the implications of eq 1 for specific cases, we make three simplifications. First, we consider contact geometries with axial symmetry between cubic materials so the
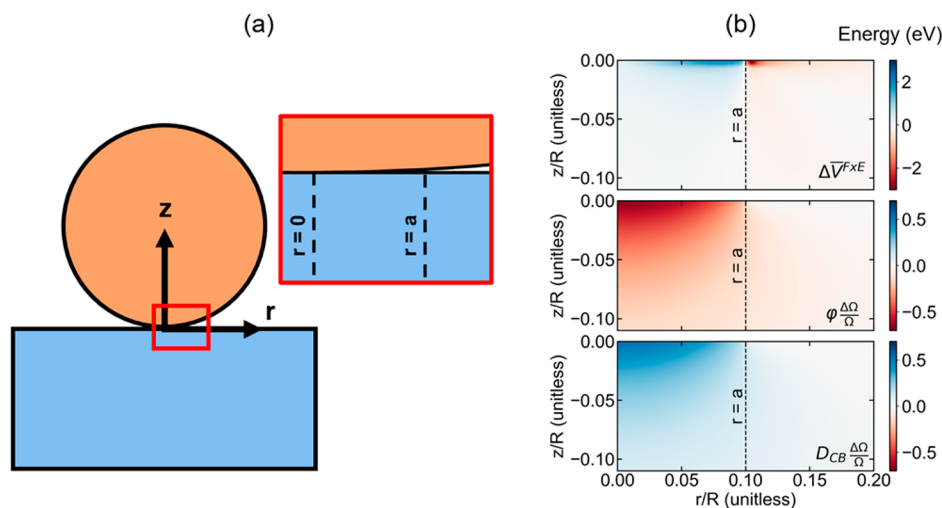
Figure 2. (a) Schematic of sphere-on-flat contact with coordinate system definition. (b) Change in the average Coulomb potential owing to flexoelectricity ($\Delta \overline{V}^{FxE}$), the average Coulomb potential relative to vacuum ($\varphi \frac{\Delta\Omega}{\Omega}$), and the conduction band minimum relative to the average Coulomb potential ($D_{CB}\frac{\Delta\Omega}{\Omega}$) in flat SrTiO$_3$ contacted by a sphere with a contact pressure of 8 GPa. Distances are normalized by the indenter radius R.

flexoelectric polarization only depends on three bulk flexo-electric coefficients. Second, we only treat volumetric strain effects in eqs 3 and 4 as shear tends to split, not shift, energy levels.[39] Third, elastic contact is assumed, which is likely a lower bound on flexoelectric contributions to triboelectricity: plastic deformation would have additional contributions from point,[40] line,[41] and planar[42] defects which are known to enhance a flexoelectric response. Materials parameters for eq 1 are calculated with density functional theory (Supporting Information), but these values could readily come from experiments. Deformation fields are determined from finite element calculations (Supporting Information) to avoid errors associated with analytic approximations (e.g., Hertz theory[43] incorrectly predicts identical deformations for contact between chemically identical bodies with different curvatures, Supporting Information). For demonstrative purposes, in this work we use SrTiO$_3$ and Si to provide concrete examples of the above framework.

Figure 2 compares the relative strengths of the three terms in eq 1 for the CB minimum in a flat SrTiO$_3$ sample deformed by a sphere with a contact pressure of 8 GPa. The deformation potential and mean-inner potential terms are largest near the contact point, decay rapidly with distance, and mostly cancel for the pressures and geometry considered here (although this is material dependent). In contrast, the flexoelectric term is concentrated near the contact radius but remains significant throughout the contact volume. The net effect is inhomogeneous band bending of ∼±1 V within the vicinity of the contact area, even for soft contact involving materials with modest flexoelectric properties such as SrTiO$_3$. The magnitude of band bending within the contact radius will monotonically increase with contact pressure (Supporting Information).

We now utilize the band bending framework developed above to construct interfacial band diagrams for sphere-on-flat contact and analyze the implications for electron charge transfer. (Contact induced band bending implications for ion transfer are discussed in the Supporting Information.) First, we analyze contact between dissimilar materials using a Si sphere and SrTiO$_3$ flat as an example. Plots of band bending at

constant pressure and different radial distances from the contact point are shown in Figure 3 and at different contact
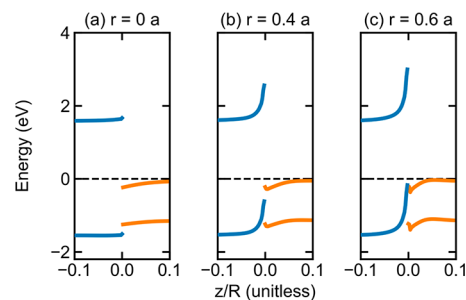

Figure 3. Sphere-on-flat contact band diagrams for a Si sphere (orange) on a SrTiO$_3$ flat (blue). (a)−(c) show the conduction and valence band edges as a function of depth (normalized by the indenter radius R) at different radial distances (in units of the contact radius a) from the contact point as defined in Figure 2a with a contact pressure of 6 GPa. The unstrained Fermi level of each material is assumed to be at its band gap center, and zero energy is taken to be the unstrained SrTiO$_3$ Fermi level.

pressures at a fixed radial distance in Figure 4. Spatially inhomogeneous band bending is observed in both bodies with the largest band bending occurring in the vicinity of the contact radius. The spatial evolution of the band bending depends sensitively on the flexoelectric coefficients; for example, there are qualitative differences in the band bending profiles of Si and SrTiO$_3$ because Si has larger shear contributions than SrTiO$_3$ (Supporting Information).

Traditional contact potential theory used to describe metal-on-metal tribocharging[8] is often deemed inapplicable to insulators because band gaps present too large an energy barrier for charge transfer.[9,14,44] Our model generalizes the theory of contact potential differences, reproducing the well-documented result that work function differences alone are insufficient to explain charge transfer in insulators, while demonstrating that band bending from elastic deformations lowers the energy barrier for transferring charge from one
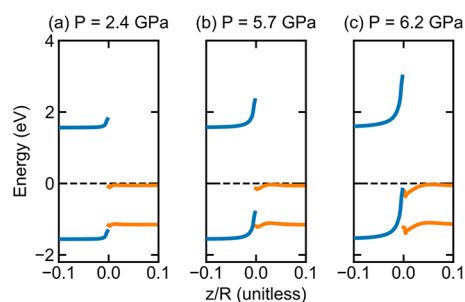
Figure 4. Sphere-on-flat contact band diagrams for a Si sphere (orange) on a SrTiO$_3$ flat (blue). (a)−(c) show the conduction and valence band edges as a function of depth (normalized by the indenter radius R) at different contact pressures for a fixed radial distance of $0.6a$ from the contact point as defined in Figure 2a. The unstrained Fermi level of each material is assumed to be at its band gap center, and zero energy is taken to be the unstrained SrTiO$_3$ Fermi level.

insulating body to another. In the limit of no in-gap states, our model predicts zero charge transfer below a contact pressure threshold (e.g., Figure 4a) followed by some transfer assuming states are available (e.g., hole transfer from the SrTiO$_3$ VB to the Si CB in Figure 4b). Sufficiently hard contact yields direct transfer between bulk states on different bodies via Zener tunneling.[45] In the example shown in Figure 4c, this corresponds to electrons tunneling from the VB of SrTiO$_3$ into the CB of Si around the edge of the contact. As mentioned earlier, reversal of the sign of charge transfer with contact pressure is well-known experimentally[16,31] but until now was unexplained; in our analysis it is a natural consequence of Zener tunneling.

In a fully adiabatic limit, the aforementioned charge transfer would be reversible; however, this limit is rarely realized. In practice there will always be in-gap states either at defects or at surfaces that trap charge so that when the two bodies return to their original configurations after contact, charge within these states (known as trapped charge and trap states, respectively) remains, leaving the materials charged. The existence of trapped charged and its relationship to triboelectricity is directly supported by triboluminescence experiments,[46,47] and the longevity of charge in trap states is well-documented.[48] Trap states have long been suggested to play an important role in triboelectricity, and some triboelectric models involve the redistribution of nonequilibrium charge distributions in localized trap states during contact.[11,12] However, the origin of the nonequilibrium distributions in these models has been an open question, and experiments suggest there is insufficient intrinsic trapped charge to explain tribocharging.[49] Our work indicates that nonequilibrium charge distributions are a natural consequence of contact: band bending arising from contact deformations reduces the energy difference between trap states and the Fermi level, providing a driving force for the occupation of trap states. Though the trap states are inherently present (e.g., from defects), they will be largely unoccupied in the absence of deformations because trap states often exist far from the Fermi level. Consequently, contact deformations may significantly increase trapped charge densities beyond intrinsic amounts, providing a possible explanation for the discrepancy between measurements of intrinsic trapped charge and transferred charge in triboelectric experiments.[49] The underlying principle in this model is analogous to increases in trapped charge densities from applied potentials observed at

semiconductor device interfaces,[50] except here trap occupation is mechanically driven.

Now we turn to sphere-on-flat contact between two SrTiO$_3$ bodies. The identical material case shown in Figure 5 is
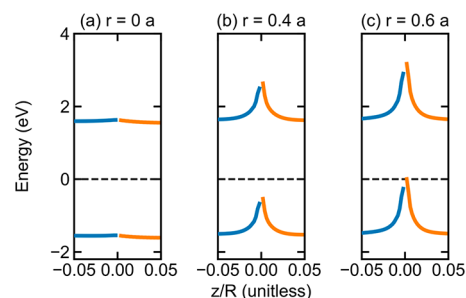

Figure 5. Sphere-on-flat contact band diagrams for a SrTiO$_3$ sphere (orange) on a SrTiO$_3$ flat (blue). (a)−(e) show the conduction and valence band edges as a function of depth (normalized by the indenter radius R) at different radial distances (in units of the contact radius a) from the contact point as defined in Figure 2a with a contact pressure of 8 GPa. The unstrained Fermi level is assumed to be at the band gap center and taken to be zero energy.

important because it models the minimal asymmetry between two bodies in which one should expect tribocharging[10] and is directly relevant for many cases such as in dust storms.[6] We note that, in the Hertzian limit, band bending during contact between two chemically identical bodies is symmetric for all combinations of curvature, so there will be no contact-deformation-driven charge transfer for two defect-free bodies; this is a known inadequacy stemming from the approximations of the Hertzian model, which is briefly recapped in the Supporting Information. When contact between two bodies is more generally treated (i.e., lifting the approximations of Hertz theory), there are subtle but important differences for contact between two bodies with different curvatures, although the differences are smaller than for dissimilar materials. Figure 5 shows asymmetric band bending across the contact interface with the largest differences around the edge of the contact region, similar to the dissimilar material case in Figure 3. For the conditions used in this simulation, there would be some transfer of electrons from the sphere to the flat, assuming states were available. Like the case involving dissimilar materials, in a fully adiabatic limit this charge transfer would be reversible, but with traps present it will not be. This result provides an explanation for the experimental observation that larger bodies tend to charge positive with respect to smaller bodies made of the same material;[49] however, our model predicts the direction of charge transfer is dictated by the relative size of the bodies and their flexoelectric coefficients. While the asymmetry between two bodies in contact with different curvatures made of identical material (Figure 5) is certainly smaller than the asymmetry between two bodies in contact made of different materials (Figure 3), the asymmetry in the former case is still on the order of 0.1 eV, which is significantly larger than thermal contributions at room temperature (0.025 eV), making it sufficient to act as a thermodynamic driver for charge transfer.

For completeness, we note that Figure 5 is strictly for the smooth limit and does not include additional roughness. To first order, the curvature will scale as $(\zeta + 1/R)$, where ζ is the roughness distribution (e.g., Gaussian) and R is the particle radius. Similar problems, albeit in the context of rough surface

contacts, have been studied in the tribological literature (e.g., refs 51−54 and references therein), and this type of approach would be needed to apply the model described in this letter to real materials—issues which we leave for future work.

In ref 22, we argued that nanoscale contact strain gradients, through flexoelectricity, are a universal driver for triboelectricity. Even with the assumptions made in that work, we were able to establish qualitative connections to a wide range of experimental triboelectric observations, but some well-established phenomena were unexplained. Here, we have solidified the theoretical basis of the hypothesis introduced in ref 22 by developing connections to *ab initio* theory and formally incorporating band structure (e.g., band gaps, band bending, deformation potentials, mean-inner potential contributions, etc.) into triboelectricity. In the process, we have explained many previously unexplained observations including the reversal of the charge transfer sign with pressure and charge transfer between spheres of identical material with different radii. Our model builds upon and incorporates older models (e.g., contact potential theory), explaining the role of materials parameters empirically known to be important but not the sole drivers of tribocharging (e.g., work function differences). In summary, the flexoelectric model for triboelectricity presented in this letter explains the following on an *ab initio* basis, with further expansion in the Supporting Information or already described:

1. Charge transfer between identical materials;[49,55−57] see also Section S3 and velocity dependence in Section S8.
2. Change in charge transfer sign with pressure;[16,31] see also Section S8
3. Work function as a component but not lone factor driving triboelectricity;[29,30] see also Sections S1 and S8.
4. Temperature dependencies through Fermi−Dirac distribution;[10,58] see also Section S1
5. Impact of the dielectric constant on tribocharging,[29,30,59] e.g., Eq 2
6. Role of trap states in electron/hole transfer;[11,12,21] see also Section S8
7. Ion transfer driven by band bending outside the contact radius;[60−63] see also Sections S7 and S8
8. Dielectric breakdown with pressure;[64] see also Section S8
9. Triboluminescence, fractoluminescence, and fractoelectrification;[46,47,65] see also Section S8

We will stress, perhaps unnecessarily, that this entire framework is rooted in the established physics of flexoelectricity, band bending, and elasticity, and there are no free parameters beyond materials parameters (which can be independently measured or calculated from first-principles). We have focused on $SrTiO_3$ and Si because they are materials with well-known properties, but there is a direct scaling for other materials. For instance, to model a hard material contacting a semiconducting polymer, one would alter the elastic constants (Supporting Information Section S5) and account for the effects of changes in the flexoelectric coefficients (Supporting Information Section S6). More work is needed on the latter point, especially in polymeric materials where the effects of chain lengths, crystallinity, and additives/fillers on flexoelectric coefficients are currently poorly understood.

That being said, there are aspects we do not specify. For instance, we do not describe the exact nature of the trap states

because these will vary with material, preparation, and gas ambient and require careful experimental work. Moving forward, it is clear that definitive matching of the band bending we predict and resultant charge transfer requires triboelectric experiments which control the number, type, and energy of defect states similar to the level of precision found in the semiconductor device community. For example, it will be important to determine the energy and spatial distribution of trap states, extent of Fermi-level pinning, nature of chemisorbed species, and/or presence of surface/interfacial dipoles which will all alter the details of the band bending. Although it will likely require large, multiscale calculations, combining these experimental details with the model described in this letter provides a platform for understanding triboelectricity and improving triboelectric applications.

The model and simulations presented in this letter demonstrate the existence of sizable inhomogeneous band bending during nanoscale contact owing to flexoelectricity, grounding the hypothesis of ref 22 in band theory, and provide a unified, *ab initio* driver for common charge transfer mechanisms. Consequences of this model are consistent with numerous experimental observations, though the detailed charge transfer mechanisms will be complex and sensitive to defects, adsorbates, etc. The framework developed here is amenable to arbitrary materials/geometries and makes sizable progress toward *a priori* predictions of triboelectric charge transfer between insulators.

■ ASSOCIATED CONTENT

🆂🅸 Supporting Information

The Supporting Information is available free of charge at https://pubs.acs.org/doi/10.1021/acs.nanolett.2c00240.

> Detailed derivation and analysis of the model used here including density functional theory and finite element calculations (PDF)

■ AUTHOR INFORMATION

Corresponding Author

Laurence D. Marks − *Department of Materials Science and Engineering, Northwestern University, Evanston, Illinois 60208, United States;* ⓘ orcid.org/0000-0002-6659-2016; Email: L-marks@northwestern.edu

Author

Christopher A. Mizzi − *Department of Materials Science and Engineering, Northwestern University, Evanston, Illinois 60208, United States*

Complete contact information is available at:
https://pubs.acs.org/10.1021/acs.nanolett.2c00240

Author Contributions

C.A.M. performed the analysis supervised by L.D.M. The manuscript was written through contributions of all authors. All authors have given approval to the final version of the manuscript.

Notes

The authors declare no competing financial interest.

■ REFERENCES

(1) Harper, W. R. *Contact and Frictional Electrification*; Oxford University Press: Oxford, 1967.

(2) Lacks, D. J; Mohan Sankaran, R Contact electrification of insulating materials. *J. Phys. D: Appl. Phys.* **2011**, *44* (45), 453001.

(3) Galembeck, F.; Burgo, T. A. L.; Balestrin, L. B. S.; Gouveia, R. F.; Silva, C. A.; Galembeck, A. Friction, tribochemistry and triboelectricity: recent progress and perspectives. *RSC Adv.* **2014**, *4*, 64280−64298.

(4) Duke, C. B.; Noolandi, J.; Thieret, T. The surface science of xerography. *Surf. Sci.* **2002**, *500*, 1005−1023.

(5) Watanabe, H.; Ghadiri, M.; Matsuyama, T.; Ding, Y. L.; Pitt, K. G.; Maruyama, H.; Matsusaka, S.; Masuda, H. Triboelectrification of pharmaceutical powders by particle impact. *Int. J. Pharm.* **2007**, *334* (1−2), 149−155.

(6) Kok, J. F.; Renno, N. O. Electrostatics in Wind-Blown Sand. *Phys. Rev. Lett.* **2008**, *100*, No. 014501.

(7) Blum, J.; Wurm, G. The Growth Mechanisms of Macroscopic Bodies in Protoplanetary Disks. *Annual Review of Astronomy and Astrophysics* **2008**, *46*, 21−56.

(8) Harper, W. R. The Voltage effect as a cause of static electrification. *Proceedings of the Royal Society A: Mathematical, Physical and Engineering Sciences* **1951**, *205* (1080), 83−103.

(9) Lacks, D. J.; Shinbrot, T. Long-standing and unresolved issues in triboelectric charging. *Nature Reviews Chemistry* **2019**, *3*, 465−476.

(10) Henry, P. S. H. The role of asymmetric rubbing in the generation of static electricity. *British Journal of Applied Physics* **1953**, *4* (S2), S31−S36.

(11) Lacks, D. J.; Duff, N.; Kumar, S. K. Nonequilibrium accumulation of surface species and triboelectric charging in single component particulate systems. *Phys. Rev. Lett.* **2008**, *100* (18), 188305.

(12) Lowell, J.; Truscott, W. S. Triboelectrification of identical insulators. II. Theory and further experiments. *Journal of Applied Physics D: Applied Physics* **1986**, *19* (7), 1281−1298.

(13) Bowden, F. P.; Tabor, D. *The friction and lubrication of solids*; Oxford University Press: New York, 1950; Vol. 1.

(14) Harper, W. R. Electrification Following the Contact of Solids. *Contemporary Physics* **1961**, *2* (5), 345−359.

(15) Helmholtz, H. Studien über electrische Grenzschichten. *Annalen der Physik* **1879**, *243* (7), 337−382.

(16) Perucca, E. Ein gründliches Experiment über die Kontakttheorie der Triboelektrizität. — Voltaeffekt erster Art und elektrische Doppelschichten beim Kontakt. *Zeitschrift für Physik* **1928**, *51* (3−4), 268−278.

(17) Harper, W. R. *Contact and Frictional Electrification*; Oxford University Press: Oxford, 1967; p 369.

(18) Baytekin, H. T.; Patashinski, A. Z.; Branicki, M.; Baytekin, B.; Soh, S.; Grzybowski, B. A. The Mosaic of Surface Charge in Contact Electrification. *Science* **2011**, *333* (6040), 308−312.

(19) Jamieson, W. The Electrification of Insulating Materials. *Nature* **1910**, *83* (2111), 189.

(20) Shaw, P. E.; Hanstock, R. F. Triboelectricity and friction. V. On surface strain and relaxation of like solids. *Proceedings of the Royal Society A: Mathematical, Physical and Engineering Sciences* **1930**, *128* (808), 474−480.

(21) Lowell, J.; Truscott, W. S. Triboelectrification of identical insulators. I. An experimental investigation. *Journal of Applied Physics D: Applied Physics* **1986**, *19* (7), 1273−1280.

(22) Sow, M.; Lacks, D. J.; Mohan Sankaran, R. Dependence of contact electrification on the magnitude of strain in polymeric materials. *J. Appl. Phys.* **2012**, *112* (8), No. 084909.

(23) Sow, M.; Widenor, R.; Kumar, A.; Lee, S. W.; Lacks, D. J.; Sankaran, R. M. Strain-Induced Reversal of Charge Transfer in Contact Electrification. *Angew. Chem.* **2012**, *124*, 2749−2751.

(24) Mizzi, C. A.; Lin, A. Y. W.; Marks, L. D. Does Flexoelectricity Drive Triboelectricity? *Phys. Rev. Lett.* **2019**, *123*, 116103.

(25) Zubko, P.; Catalan, G.; Tagantsev, A. K. Flexoelectric Effect in Solids. *Annu. Rev. Mater. Res.* **2013**, *43*, 387−421.

(26) Burgo, T. A.; Erdemir, A. Bipolar tribocharging signal during friction force fluctuations at metal-insulator interfaces. *Angew. Chem., Int. Ed.* **2014**, *53* (45), 12101−12105.

(27) Xu, C.; Zhang, B.; Wang, A. C.; Zou, H.; Liu, G.; Ding, W.; Wu, C.; Ma, M.; Feng, P.; Lin, Z.; Wang, Z. L. Contact-Electrification between Two Identical Materials: Curvature Effect. *ACS Nano* **2019**, *13*, 2034−2041.

(28) Persson, B. N. J. On the role of flexoelectricity in triboelectricity for randomly rough surfaces. *Europhys. Lett.* **2020**, *129*, 10006.

(29) Davies, D. K. Charge generation on dielectric surfaces. *J. Phys. D: Appl. Phys.* **1969**, *2* (11), 1533−1537.

(30) Zou, H.; Guo, L.; Xue, H.; Zhang, Y.; Shen, X.; Liu, X.; Wang, P.; He, X.; Dai, G.; Jiang, P.; Zheng, H.; Zhang, B.; Xu, C.; Wang, Z. L. Quantifying and understanding the triboelectric series of inorganic non-metallic materials. *Nat. Commun.* **2020**, *11*, 2093.

(31) Baytekin, H. T.; Baytekin, B.; Incorvati, J. T.; Grzybowski, B. A. Material transfer and polarity reversal in contact charging. *Angew. Chem., Int. Ed.* **2012**, *51* (20), 4843−4847.

(32) Mott, N. F. The Theory of Crystal Rectifiers. *Proceedings of the Royal Society of London. Series A, Mathematical and Physical Sciences* **1939**, *171* (944), 27−38.

(33) Schottky, W. Zur Halbleitertheorie der Sperrschicht- und Spitzengleichrichter. *Zeitschrift für Physik* **1939**, *113*, 367−414.

(34) Halasyamani, P. S.; Poeppelmeier, K. R. Noncentrosymmetric Oxides. *Chem. Mater.* **1998**, *10*, 2753−2769.

(35) Stengel, M. Surface control of flexoelectricity. *Phys. Rev. B* **2014**, *90*, 201112.

(36) Mizzi, C. A.; Marks, L. D. The Role of Surfaces in Flexoelectricity. *J. Appl. Phys.* **2021**, *129* (22), 224102.

(37) Bardeen, J.; Shockley, W. Deformation Potentials and Mobilities in Non-Polar Crystals. *Phys. Rev.* **1950**, *80* (1), 72−80.

(38) Shockley, W.; Bardeen, J. Energy Bands and Mobilities in Monatomic Semiconductors. *Phys. Rev.* **1950**, *77* (3), 407−408.

(39) Van de Walle, C. Band lineups and deformation potentials in the model-solid theory. *Phys. Rev. B* **1989**, *39* (3), 1871−1883.

(40) Narvaez, J.; Vasquez-Sancho, F.; Catalan, G. Enhanced flexoelectric-like response in oxide semiconductors. *Nature* **2016**, *538* (7624), 219−221.

(41) Gao, P.; Yang, S.; Ishikawa, R.; Li, N.; Feng, B.; Kumamoto, A.; Shibata, N.; Yu, P.; Ikuhara, Y. Atomic-Scale Measurement of Flexoelectric Polarization at SrTiO3 Dislocations. *Phys. Rev. Lett.* **2018**, *120*, 267601.

(42) Mizzi, C. A.; Guo, B.; Marks, L. D. Twin-Boundary-Mediated Flexoelectricity in LaAlO3. *Physical Review Materials* **2021**, *5*, No. 064406.

(43) Hertz, H. Über die Berührung fester elastischer Körper. *Journal fur die Reine und Angewandte Mathematik* **1882**, *1882* (92), 156−171.

(44) Harper, W. R. Contact Electrification of Semiconductors. *British Journal of Applied Physics* **1960**, *11* (8), 324−331.

(45) Zener, C. A Theory of the Electrical Breakdown of Solid Dielectrics. *Proceedings of the Royal Society A: Mathematical, Physical and Engineering Sciences* **1934**, *145* (855), 523−529.

(46) Walton, A. J. Triboluminescence. *Adv. Phys.* **1977**, *26* (6), 887−948.

(47) Zink, J. I. Triboluminescence. *Acc. Chem. Res.* **1978**, *11* (8), 289−295.

(48) Randall, J. T.; Wilkins, M. H. F. Phosphorescence and electron traps II. The interpretation of long-period phosphorescence. *Proceedings of the Royal Society A: Mathematical, Physical and Engineering Sciences* **1945**, *184* (999), 390−407.

(49) Waitukaitis, S. R.; Lee, V.; Pierson, J. M.; Forman, S. L.; Jaeger, H. M. Size-Dependent Same-Material Tribocharging in Insulating Grains. *Phys. Rev. Lett.* **2014**, *112* (21), 218001.

(50) Mikheev, E.; Hoskins, B. D.; Strukov, D. B.; Stemmer, S. Resistive switching and its suppression in Pt/Nb:SrTiO3 junctions. *Nat. Commun.* **2014**, *5*, 3990.

(51) Greenwood, J. A.; Tripp, J. H. Elastic Contact of Rough Spheres. *Journal of Applied Mechanics* **1967**, *34* (1), 153−159.

(52) Persson, B. N.; Albohr, O.; Tartaglino, U.; Volokitin, A. I.; Tosatti, E. On the nature of surface roughness with application to contact mechanics, sealing, rubber friction and adhesion. *J. Phys.: Condens. Matter* **2005**, *17* (1), R1−R62.

(53) Mulakaluri, N.; Persson, B. N. J. Adhesion between elastic solids with randomly rough surfaces: Comparison of analytical theory with molecular-dynamics simulations. *Epl* **2011**, *96* (6), 66003.

(54) Pastewka, L.; Robbins, M. O. Contact area of rough spheres: Large scale simulations and simple scaling laws. *Appl. Phys. Lett.* **2016**, *108* (22), 221601.

(55) Forward, K. M.; Lacks, D. J.; Sankaran, R. M. Charge segregation depends on particle size in triboelectrically charged granular materials. *Phys. Rev. Lett.* **2009**, *102* (2), No. 028001.

(56) Pham, R.; Virnelson, R. C.; Sankaran, R. M.; Lacks, D. J. Contact charging between surfaces of identical insulating materials in asymmetric geometries. *J. Electrost.* **2011**, *69* (5), 456−460.

(57) Shinbrot, T.; Komatsu, T. S.; Zhao, Q. Spontaneous tribocharging of similar materials. *Europhys. Lett.* **2008**, *83* (2), 24004.

(58) Xu, C.; Zi, Y.; Wang, A. C.; Zou, H.; Dai, Y.; He, X.; Wang, P.; Wang, Y.-C.; Feng, P.; Li, D.; Wang, Z. L. On the Electron-Transfer Mechanism in the Contact-Electrification Effect. *Adv. Mater.* **2018**, *30*, 1706790.

(59) Rose, G. S.; Ward, S. G. Contact electrification across metal-dielectric and dielectric-dielectric interfaces. *British Journal of Applied Physics* **1957**, *8*, 121−126.

(60) Harris, I. A.; Lim, M. X.; Jaeger, H. M. Temperature dependence of nylon and PTFE triboelectrification. *Physical Review Materials* **2019**, *3*, No. 085603.
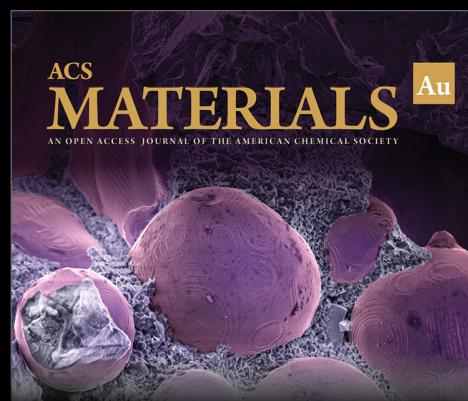
(61) Lee, V.; James, N. M.; Waitukaitis, S. R.; Jaeger, H. M. Collisional charging of individual submillimeter particles: Using ultrasonic levitation to initiate and track charge transfer. *Physical Review Materials* **2018**, *2*, No. 035602.

(62) McCarty, L. S.; Whitesides, G. M. Electrostatic Charging Due to Separation of Ions at Interfaces: Contact Electrification of Ionic Electrets. *Angew. Chem.* **2008**, *47*, 2188−2207.

(63) Zhang, Z.; Yates, J. T. Band Bending in Semiconductors: Chemical and Physical Consequences at Surfaces and Interfaces. *Chem. Rev.* **2012**, *112* (10), 5520−5551.

(64) Jeffery, S.; Sofield, C. J.; Pethica, J. B. The influence of mechanical stress on the dielectric breakdown field strength of thin SiO2 films. *Appl. Phys. Lett.* **1998**, *73* (2), 172−174.

(65) Chandra, B. P.; Chandra, V. K.; Jha, P.; Patel, R.; Shende, S. K.; Thaker, S.; Baghel, R. N. Fracto-mechanoluminescence and mechanics of fracture of solids. *J. Lumin.* **2012**, *132* (8), 2012−2022.